Near-Field Phase Reconstruction for UAV-based Antenna Measurements

L. Ciorba[1,2] , G. Virone[1], F. Paonessa[1], S. Matteoli[1], P. Bolli[3], E. de Lera Acedo[4], N. Razavi Ghods[4], J. Abraham[5], E. Colin Beltrán[6], K. Zarb Adami[7], A. Magro[8], O. A. Peverini[1], G. Addamo[1], G. Giordanengo[9], M. Righero[9], G. Vecchi[2].

[1]Institute of Electronics, Computer and Telecommunication Engineering (IEIIT-CNR), Torino, Italy; e-mail address*

[2]Department of Electronics and Telecommunications, Politecnico di Torino, Torino, Italy; giuseppe.vecchi@polito.it

[3]National Institute of Astrophysics (INAF), Astronomical Observatory of Arcetri, Florence, Italy; pbolli@arcetri.inaf.it

[4]Cavendish Laboratory, Cambridge, United Kingdom; {eloy,nima}@mrao.cam.ac.uk

[5]Department of Electronic Systems, Norwegian University of Science and Technology, Trondheim, Norway; jens.abraham@ntnu.no

[6]Conacyt, Instituto Nacional de Astrofisica, Optica y Electronica, Tonantzintla, Puebla, Mexico; edgarcb@inaoep.mx

[7]University of Oxford, Department of Physics, Oxford, United Kingdom; kza@astro.ox.ac.uk

[8]Institute of Space Sciences and Astronomy, University of Malta, Malta; alessio.magro@um.edu.mt

[9]Antenna and EMC Lab, Istituto Superiore Mario Boella (ISMB), Torino, Italy; {giordanengo,righero}@ismb.it

*{lorenzo.ciorba, giuseppe.virone, fabio.paonessa, stefania.matteoli, oscar.peverini, giuseppe.addamo}@ieiit.cnr.it

***Abstract*—A non-tethered Unmanned Aerial Vehicle equipped with a RF source has been used as a near-field scanner in the VHF band. In this configuration, the source is not phase-locked to the receiver local oscillator/clock. A reference antenna, placed at a proper distance from the antenna-under-test, has thus been exploited to reconstruct the phase. Experimental results at 175 MHz for the central element of the Pre Aperture Array Verification System of the Square Kilometre Array are shown. The comparison with simulations shows very good agreement.**

***Index Terms*—Antenna measurements, near-field measurements, unmanned aerial vehicle.**

I. Introduction

In recent years, radiation pattern measurements based on Unmanned Aerial Vehicles (UAVs) have been performed on a variety of radio astronomical facilities and prototypes such the Low-Frequency Array (LOFAR) [1],[2], the Square Kilometer Array Aperture Array Verification System (SKA-AAVS) [3] and the Medicina Array Demonstrator [4],[5]. An UAV equipped with a radio-frequency test source [6] and a differential Global Navigation Satellite System (GNSS) positioning device was mainly placed in the far-field of antenna arrays in order to characterize their radiation pattern exploiting a variety of scan strategies [7]. As far as the LOFAR telescope is concerned [2], the far-field condition could not be reached owing to its large overall size. In that case, the UAV performed a few near-field linear scans over the telescope and the acquired data were successfully compared to simulation performed in the same regime [2]. A near- to far-field (NF-to-FF) transformation was not possible on the LOFAR data due to the lack of phase information and the limited amount of linear scans, i.e. the aperture was not fully sampled. In the literature, phase-less techniques have been already applied to UAV-collected data [8]. Other researches have proposed a fiber-optic link between the UAV and ground to recover the phase information in order to perform a NF-to-FF transformation with an inverse-source approach [9]. In this paper, an alternative solution exploiting an additional reference antenna on the ground is proposed and verified. In this way, the UAV is not tethered to ground so that there are no limitations on its scan strategy and there is no additional weight contribution from attached cables.

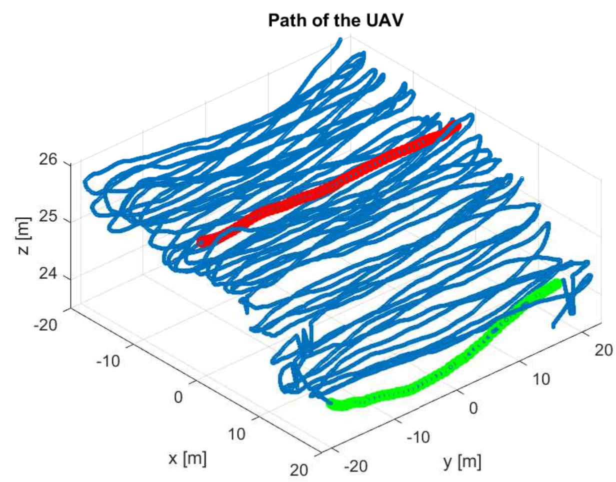

Fig. 1. Example of UAV trajectory during a near-field scan (blue curve). Trajectories selected for comparison between reconstructed and simulated phases (red and green markers).

II. Example of near-field scan

Figure 1 shows an example of UAV trajectory measured with a differential GNSS system (centimetrical accuracy). The programmed flight was actually set as a regular planar

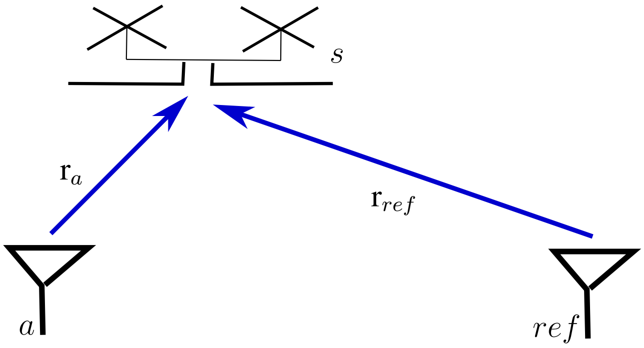

Fig. 2. Measurement schematics: the UAV (s) and the reference antenna (*ref*) are in far-field condition while s is in the near-field of the AUT (a). Position vectors $\mathbf{r}_a$, $\mathbf{r}_{ref}$ are considered with respect to a reference system centered in a and *ref*, respectively.

raster with a constant height of 25 m and constant line spacing of about 0.7 m. As a matter of fact, the presented UAV trajectory is quite irregular and far from the planned measurement path. It can be envisaged that classical near-field to far-field transformations are hardly applicable in this case. On the contrary, inverse source methods [10],[11],[12] could be exploited owing to their capability of dealing with arbitrary sample distributions. In both classical and inverse-source methods, the phase information always provides better accuracy and faster reconstruction, i.e. less number of samples. However, the phase knowledge is challenging for UAV-based measurements because the synthesizer on-board is not phase-locked to the receiving equipment. Section III reports that the phase information can be retrieved by means of a reference antenna placed at a certain distance from the Antenna Under Test (AUT) (Figure 2). This technique is applied to experimental data and compared to simulations in Section IV.

III. Phase Reconstruction

Figure 2 shows the measurement scheme that is used to reconstruct the phase difference

$$\Delta\varphi_{as} = \varphi_a - \varphi_s \tag{1}$$

where φ_a is the phase of the received voltage measured at the AUT port, whereas φ_s is the phase of the transmitted signal from the UAV (which is unknown). It should be noted that $\Delta\varphi_{as}$ is the phase information required to perform NF-to-FF transformations.

The proposed technique requires the usage of a two-channel receiver on the ground. Depending on the operative frequency and bandwidth, several options are available based on either direct sampling of the RF signal [3] or with a first down-conversion stage. The two-port receiver performs the measurement of complex voltages at both the AUT (a) and the reference antenna (*ref*) ports.

The reference antenna has to be placed far from the array in order to be considered as an isolated element that is not interacting with it. Moreover, the far-field condition between the UAV and the reference antenna should be satisfied. Under these hypotheses, the measured phase at the reference antenna port can be expressed as

$$\varphi_{ref}(\mathbf{r}_{ref}) = \varphi_s - k|\mathbf{r}_{ref}| + \lfloor(\mathbf{p}_{ref}(\hat{\mathbf{r}}_{ref}) \cdot \mathbf{p}_s(\hat{\mathbf{r}}_{ref})) \tag{2}$$

where k is the wavenumber, $\mathbf{p}_{ref}$ and $\mathbf{p}_s$ are the polarization unit vectors of the reference antenna and source respectively (i.e. $\mathbf{p}(\hat{\mathbf{r}}) = \mathbf{E}(\hat{\mathbf{r}})/|\mathbf{E}(\hat{\mathbf{r}})|$ where $\mathbf{E}$ is the E-field pattern), $\mathbf{r}_{ref}$ is the position vector of the source with respect to the reference antenna, the symbol $\lfloor$ denotes the phase of a complex number; the hat symbol denotes unit direction vectors. It should be noted that the second term on the right hand side of (2) is the propagation phase between source and reference, whereas the last term of (2) is the phase of the polarization mismatch. The propagation phase can be estimated using the measured position of the source. The polarization mismatch can be instead estimated from the knowledge of both source and reference radiation pattern. In these conditions, it is apparent that the phase of the source signal φ_s can be estimated from the measured φ_{ref}. Finally, by substituting (2) into (1), the required $\Delta\varphi_{as}$ can be retrieved as

$$\begin{aligned}\Delta\varphi_{as}(\mathbf{r}_a) = \varphi_a(\mathbf{r}_a) - \varphi_{ref}(\mathbf{r}_{ref}) - k|\mathbf{r}_{ref}| + \\ + \lfloor(\mathbf{p}_{ref}(\hat{\mathbf{r}}_{ref}) \cdot \mathbf{p}_s(\hat{\mathbf{r}}_{ref}))\end{aligned} \tag{3}$$

where $\mathbf{r}_a$ is the position vector of the source with respect to the AUT (Figure 2). Of course, $\mathbf{r}_a$ and $\mathbf{r}_{ref}$ are univocally related to each other since they represent the source position in two different reference systems.

Equations (2) and (3) are valid up to addition by a constant that depends on the receiver calibration. Such a constant does not depend on the position of the source.

The same measurement scheme is generally applied in common far-field test ranges. In this case, however, the relative distance $|\mathbf{r}_{ref}|$ between source and reference is kept constant so that knowledge of $\mathbf{r}_{ref}$, $\mathbf{p}_{ref}$ and $\mathbf{p}_s$ is not required.

IV. Experimental Results

A set of near-field flights has been performed on the Pre Aperture Array Verification System (Pre -AAVS1) [3] of the Square Kilometre Array located at the Mullard Observatory in Cambridge (UK). Such an array is composed of 16 active dual-pol log-periodic elements oriented at zenith and arranged in a random configuration with a maximum distance from the center of about 4 m. In order to test the presented phase reconstruction technique, another log-periodic antenna has been placed at 20 m from the array center and used as reference antenna. All the antenna elements were connected to the back-end unit by means of coaxial cables.

In this Section, the phase reconstruction method is applied to the UAV flight shown in Fig. 1, for which the source frequency was set to 175 MHz. The results are presented for the array element that is closer to the center.

According to (3), φ_a and φ_{ref} are measured data obtained from the digital back-end. The relative position data are obtained from measured differential GNSS data. The quantities

$\mathbf{p}_s(\hat{\mathbf{r}}_{ref})$ and $\mathbf{p}_{ref}(\hat{\mathbf{r}}_{ref})$ are instead evaluated from look-up-tables of the source and reference antenna patterns, respectively. In this case, the look-up-tables have been computed with FEKO. In principle, measured patterns could be used, however, a complete set of data cannot be easily achieved at VHF frequencies. Verifications of the used look-up-tables have been already performed in [3] and [13].

The reconstructed phase $\Delta\varphi_{as}$ over the whole path of Fig. 1 is shown in Fig. 3. The UAV-mounted dipole was mainly oriented along the y-axis in Fig. 1, which is the same polarization of the considered array-element under test. The overall phase distribution looks consistent with the radiated field from a small antenna in the proximity of the array center.

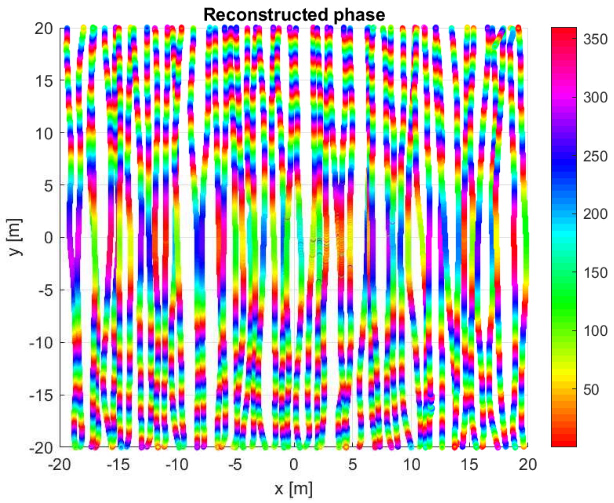

Fig. 3. Near-field Phase reconstruction (y-component) for the array element that is closer to the center. The 3-D trajectory of the source is shown in Fig. 1.

The reconstructed phase $\Delta\varphi_{as}$ along the flying trajectories with red and green markers in Fig. 1 is compared to FEKO simulations in Figs. 4 and 5, respectively. The overall agreement is very good. The unknown constant (see above) has been selected to minimize the distance between reconstruction and simulation. The residual average error between measurements and simulation is 7° and 13.5°, respectively.

V. Conclusion

A method for reconstructing the phase for near-field UAV-based scans has been presented. The phase of the co-polar component of the electric field for an embedded element has been reconstructed at 175 MHz in order to demonstrate the applicability of the method. It showed good consistency with the simulated data. This encourages the exploitation of inverse-source techniques [11],[12] in order to compute the far-field pattern from the near-field data.

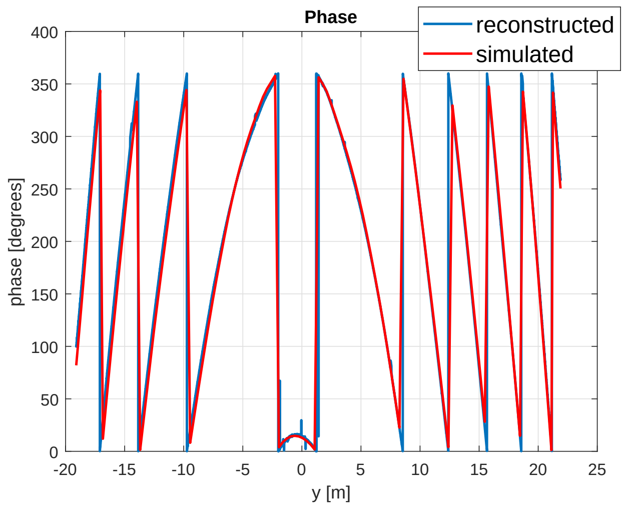

Fig. 4. Reconstructed (blue curve) and simulated phase (red curve) of $y-$component of the AUT near-field along the red trajectory in Fig. 1.

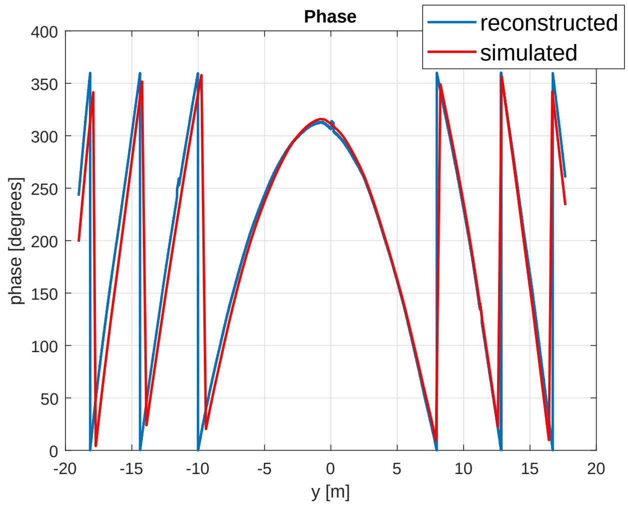

Fig. 5. Reconstructed (blue curve) and simulated phase (red curve) of $y-$component of the AUT near-field along the green trajectory in Fig. 1.

Acknowledgment

The authors would like to thank Andrea Lingua, Paolo Maschio, Marco Piras (Department of Environment, Land and Infrastructure Engineering, Politecnico di Torino, Torino, Italy) and Augusto Olivieri (Institute of Electronics, Computer and Telecommunication Engineering IEIIT-CNR, Torino, Italy) for their valuable support.

References

[1] G. Virone et al. - *Strong Mutual Coupling Effects on LOFAR: Modeling and In Situ Validation*, IEEE Transactions on Antennas and Propagation, vol. 66(5), May 2018.

[2] P. Bolli et al. - *Near-field Experimental Verification of the EM Models for the LOFAR Radio Telescope*, IEEE Antennas and Wireless Propagation Letters, vol. 17(4), April 2018.

[3] E. de Lera-Acedo et al. - *SKA aperture array verification system: electromagnetic modeling and beam pattern measurements using a micro UAV* , Experimental Astronomy, vol. 45, 1, 2018.

[4] G. Pupillo et al. - *Medicina Array Demonstrator: calibration and radiation pattern characterization using a UAV-mounted radio-frequency*

source, Experimental Astronomy, vol. 39, issue 2, pp. 405-421, June 2015. DOI: 10.1007/s10686-015-9456-z

[5] P. Bolli et al. - *From MAD to SAD: the Italian experience for the Low Frequency Aperture Array of SKA1-LOW*,", Radio Science, vol. 51, issue 3, pp. 160–175, Mar. 2016. DOI: 10.1002/2015RS005922

[6] G. Virone et al. - *Antenna Pattern Verification System Based on a Micro Unmanned Aerial Vehicle (UAV)*, IEEE Antennas and Wireless Propagation Letters, vol. 13, 2014.

[7] F. Paonessa et al. - *UAV-based antenna measurements: Scan strategies*, 11th European Conference on Antennas and Propagation (EUCAP), 2017.

[8] M. G. Fernandez et al. - *Antenna Diagnostics and Characterization using Unmanned Aerial Vehicles*, IEEE Access (Volume: 5), 2017.

[9] T. Fritzel et al. - *Introduction into an UAV-based near-field system for in-situ and large-scale antenna measurements*, IEEE Conference on Antenna Measurements & Applications (CAMA), 2016.

[10] G. Giordanengo, M. Righero, F. Vipiana, G. Vecchi, M. Sabbadini - *Fast Antenna Testing with Reduced Near Field Sampling*, IEEE Transactions on Antennas and Propagation, 62(5):2501–2513, May 2014.

[11] M. Righero et al. - *Near-Field to Far-Field transformation using data acquired with an Unmanned Aerial Vehicle*, IEEE International Symposium on Antennas and Propagation and USNC-URSI Radio Science Meeting, 2018.

[12] M. Righero et al. - *A method to evaluate the far-field pattern from scattered near-field data acquired with an unmanned aerial vehicle*, International Conference on Electromagnetics in Advanced Applications (ICEAA), 2018.

[13] G. Virone et al. - *Antenna pattern measurement with UAVs: Modeling of the test source*, 2016 10th European Conference on Antennas and Propagation (EuCAP), Davos, 2016, pp. 1-3. doi: 10.1109/EuCAP.2016.7481744